

Electronic Implementation of the Mackey-Glass Delayed Model

Pablo Amil, Cecilia Cabeza, Arturo C. Martí

Abstract—The celebrated Mackey-Glass model describes the dynamics of physiological *delayed* systems in which the actual evolution depends on the values of the variables at some *previous* times. This kind of systems are usually expressed by delayed differential equations which turn out to be infinite-dimensional. In this contribution, an electronic implementation mimicking the Mackey-Glass model is proposed. New approaches for both the nonlinear function and the delay block are made. Explicit equations for the actual evolution of the implementation are derived. Simulations of the original equation, the circuit equation, and experimental data show great concordance.

Index Terms—Delayed circuits, Mackey-Glass, Experimental chaos.

I. INTRODUCTION

In 1977, a paper entitled *Oscillation and Chaos in Physiological Control Systems* [1] was published in *Science*. This paper, by Michael C. Mackey and Leon Glass (MG), dealt with physiological processes, mainly respiratory and hematopoietic (*i.e.* formation of blood cellular components) diseases in which time delays play a significant role. In effect, in the production of blood cells there is a considerable delay between the initiation of cellular production in the bone marrow and the release into the blood. In general, in these processes, the evolution of the system at a given time not only depends on the state of the system at the current time but also on the state of the system at *previous* times. The MG's work had an impressive impact. Since its publication, it exhibits nearly 3000 cites in scientific journals and, at present, Google reports more than two millions results for the search *Mackey-Glass*.

In their pioneering paper, Mackey and Glass showed that a variety of physiological systems can be adequately described in terms of simple nonlinear delay-differential equations. The model proposed by MG exhibits a wide range of behaviors including periodic or chaotic solutions. The importance of the MG model lies in the fact that the onset of some diseases are associated with alterations in the periodicity of certain physiological variables, for example, irregular breathing patterns or fluctuations in peripheral blood cell counts.

The dynamics of processes involving time delays as those studied by MG is far more complex than non-delayed, *i.e.*, instantaneous systems. Actually, if the dynamics of a system at time t depends on the state of the system at time $t - \tau$, the information needed to predict the evolution is content in the whole interval $(t - \tau, t)$. Thus, the evolution of a delayed system depends on *infinite* previous values of the variables.

Pablo Amil, Cecilia Cabeza, and Arturo C. Martí are with the Physics Institute, Universidad de la República, Iguá 4225, Montevideo, Uruguay, (see <http://www.fisica.edu.uy>).

Manuscript received —, 2014; revised —, 2014.

From the mathematical point of view, delayed systems are modelled in terms of delayed differential equations (DDEs) and one single DDE is equivalent to infinite ordinary differential equations (ODEs). Due to their infinite dimensionality, the accuracy of numerical simulations of DDEs is specially delicate. In practice, this problem is avoided considering large transients. However, there persist doubts about the stability and accuracy of the methods used to numerically integrate DDEs.

Thank to its richness in behaviors, the Mackey-Glass model has acquired relevance of its own [2], [3], [4], [5], [6]. One direct application is using MG model as a simple way to generate a chaotic signal [7], [8] to be used in multiple ways as for example to check methods to characterize chaotic measures or stability schemes [9], [6].

Several electronic implementations of MG model have been proposed [10], [9], [6], [11], [12]. In Ref. [9], an electronic implementation based on an *analog delay line* was proposed to address the problem of controlling high dimensional chaos in infinite dimensional system. The focus was on the stabilization of unstable steady states (USS) in a electronic analog to the MG system. A possible application of the MG model is to employ several delayed values of the variable $x(t - \tau_1)$, $x(t - \tau_2)$, $x(t - \tau_3)$... instead of only one [5], [12]. More specifically, Taneto and Uchida [12], investigated the generation of chaos in a Mackey-Glass electronic circuit with two time-delayed feedback loops observing different dynamical behaviors when the two delay times were changed. The ratio of the two time delays was found crucial to enhance or suppress the chaotic dynamics. The synchronization of chaos in unidirectionally-coupled Mackey-Glass electronic circuits with two time delays was also investigated confirming that synchronization of chaos can be achieved even in the presence of the two time-delayed feedback loops. High-quality synchronization of chaos can be achieved at the strong coupling strengths and parameter matching conditions between the two circuits.

The goal of this paper is to propose a novel electronic implementation of the Mackey-Glass system. We show how this implementation approximates the original equation by deriving its evolution equation. Then we show results of simulations comparing the original Mackey-Glass equation and the effective circuit equation with the experimental data, which all show great agreement between each other.

This paper is organized as follows. Section II deals specifically with the design of the circuit. We pay special attention to the delay block and the function block which implement the nonlinear term. In Sec. III we derive the governing equation of the designed circuit. For this circuit, in Sec. IV we present both, numerical and experimental results. Finally, in Sec. V we draw our conclusions.

II. THE MODEL AND ITS ELECTRONIC IMPLEMENTATION

Let us consider the production of blood cells. The homogeneous density of a population of mature circulating cells is denoted P . As mentioned before, there is a significant delay τ between the initiation of cellular production in the bone marrow and the release into the blood. According to Ref. [1] (Eq. 4b), the delay differential equation governing the evolution of the population is

$$\frac{dP}{dt} = \frac{\beta_0 \Theta^n P_\tau}{\Theta^n + P_\tau^n} - \gamma P, \quad (1)$$

where $P_\tau(t) = P(t - \tau)$. The parameters β_0 , Θ , and n are related to the production rate while γ determines the decay rate of the cells.

To simplify the Eq. 1, we will reduce it to an equivalent equation with less model parameters. To that end, we will define a new state-variable and a new independent-variable as $x = P/\Theta$ and $t' = \gamma t$ respectively. We also define new parameters such that $\Gamma = \gamma\tau$ and $\alpha = \beta_0/\gamma$. Thus, the Eq. 1 can be now written as

$$\frac{dx}{dt'} = \alpha \frac{x_\Gamma}{1 + x_\Gamma^n} - x \quad (2)$$

being $x_\Gamma(t') = x(t' - \Gamma)$. The electronic implementation will mimic this equation by properly setting α and Γ .

Concerning the dynamics of the MG model given by Eqs. 1 or 2, the role of the time delay τ is crucial. For the instantaneous system, $\tau = 0$, depending on the parameter values, there is only one positive stable fixed point. However, as τ , is increased, the initially stable equilibrium point becomes unstable and periodic solutions appear [6]. If τ is further increased a sequence of bifurcations gives place to oscillations with higher periods and aperiodic behavior. The value of n considered in [1] was $n = 10$, but similar behaviors can be seen with other values of n [2].

A. Block diagram

The electronic implementation was divided in two main parts: the delay block, which presents only a time shift between its input and its output; and the function block, which implements the nonlinear term of the equation. After having these blocks the complete circuit looks as in Fig. 1. In this scheme the function block implements the first term in the r.h.s. of Eq. 1 or Eq. 2 without delay

$$f(v) = \beta \frac{v}{\theta^n + v^n}, \quad (3)$$

and the delay block implements the transfer function:

$$v_{out}(t) = v_{in}(t - \tau). \quad (4)$$

Assuming ideal behavior of both blocks, the equation for the potential at the capacitor terminals is given by

$$\frac{dv_c(t)}{dt} = \frac{1}{RC} [f(v_c(t - \tau)) - v_c(t)] \quad (5)$$

which can be identify with Eq. 2 by setting $t' = t/RC$, $x = v_c/\theta$, $\Gamma = \tau/RC$, and $\alpha = \beta/\theta^n$.

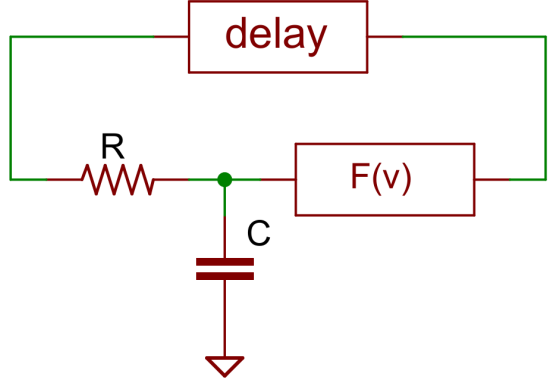


Fig. 1. Block schematic of the complete circuit: delay and nonlinear function blocks, with the RC

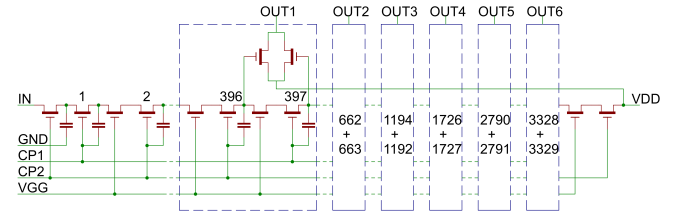


Fig. 2. Internal structure of a Bucket Brigade Device (BBD)

B. Delay block

The purpose of the delay block is to copy the input to the output after some time delay. The implementation of this block with analog electronic is possible using a Bucket Brigade Device (BBD), which is a discrete-time analog device, internally it consists of an array of N capacitors in which the signal travels one step at a time, as shown in Fig. 2. In our implementation we used the integrated circuits MN3011 and MN3101 as BBD and clock signal generator respectively.

This approach of implementing a delay approximates the desired transfer function given by Eq. 4, by sampling the input signal and outputting those samples N clock periods later. The effective transfer equation is the following

$$v_{out}(t) = g_d v_{in} \left(T_s \left\lfloor \frac{t}{T_s} - N + 1 \right\rfloor \right) + V_d \quad (6)$$

where T_s is the sampling period of the BBD, and N is the number of capacitors in the array, g_d and V_d stand for gain and offset voltage introduced by the BBD respectively. The symbols $\lfloor \cdot \rfloor$ stand for the integer part. In the MN3011 the sampling period can vary between $5\mu s$ and $50\mu s$. The number of capacitors in the array, N , can be selected among the values provided by the manufacturer ($N = 396, 662, 1194, 1726, 2790, 3328$). An example of its functionality can be seen in Fig. 3 where, to fully appreciate the input and output signals, the offset and the gain are null and a simulated value of N (non provided by the manufacturer) is employed.

In order to avoid the effects of offset and gain, and also to expand the intrinsic dynamic range of the BBD (originally between 0 V and 4 V), the complete delay block included pre-

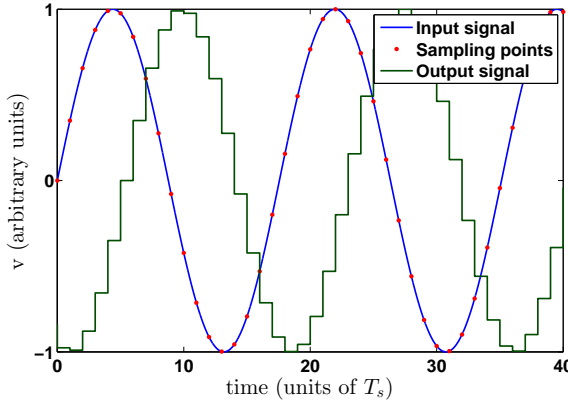


Fig. 3. Simulated example of input and output signals of a BBD and sampling points. For the sake of clarity, the offset and gain are null and $N = 5$.

and post-amplification and offset adjust as shown in Fig. 4. The delay was set to 10 ms using $N = 1194$. All trimmers in the circuit were adjusted to obtain a dynamic range between 0 V and 10 V, and a transfer equation as follows

$$v_{out}(t) = v_{in} \left(T_s \left\lfloor \frac{t}{T_s} - N + 1 \right\rfloor \right). \quad (7)$$

Input and output test signals are shown in Fig. 5.

It is worth noting that, due to its internal clock, a certain amount of high-frequency noise is introduced by the delay block. This is the reason that explains the ordering of the blocks in which the delay block is after the function block and immediately before the RC circuit. With this configuration, most of this noise is suppressed.

C. Function block

The function block was implemented for $n = 4$, as shown in the circuit schematics in Fig. 6. Other values of the exponent n could be similarly implemented. Assuming all the operational amplifiers are working in the linear region, the transfer function results as in Eq. 3 by defining $\theta = k_1 ad^{\frac{1}{4}}$ and $\beta = k_2 b^{\frac{1}{4}}$ where k_1 and k_2 are constants that depend on the circuit and a , b and d depend on the positions of the trimmers indicated in Fig. 6. The parameter a does not depend on the dimensionless parameters that determine the evolution of the system, α and Γ , but only depends on θ that sets the amplitude of the oscillations. Therefore a can be set to avoid all kind of saturation in the circuit without changing the dynamical properties of the oscillations.

Integrated circuits AD633JN and AD712JN were used to implement sums, multiplications and divisions because of their simplicity, accuracy, low noise and low offset voltage. In Fig. 7, an input-output graph of this block is depicted and compared with Eq. 3. Although it was tested from -10 V to 10 V, it is used only with positive voltages as they are the only relevant in the MG model.

III. EFFECTIVE EQUATION

Since the delay block we used approximates an ideal delay, the effective equation of the implemented circuit will also

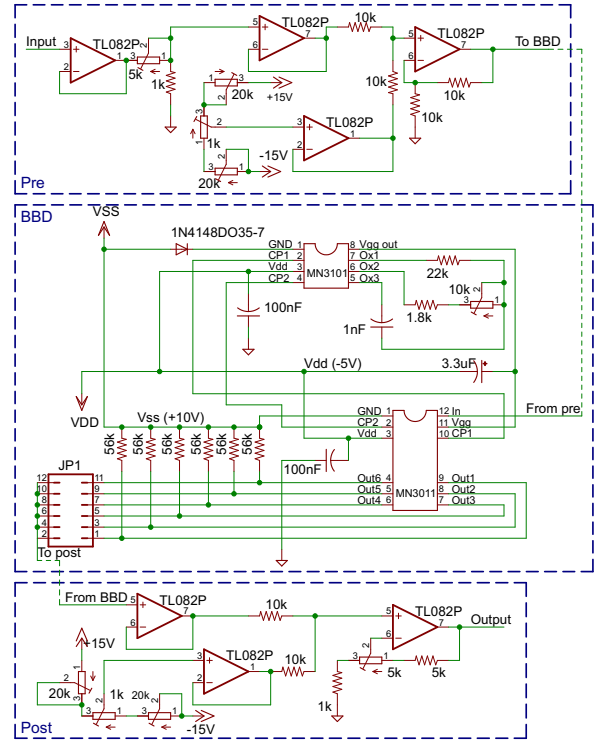


Fig. 4. Circuit schematic of the delay block. The blue-dashed boxes correspond to the pre-amplification, BBD and post-amplification.

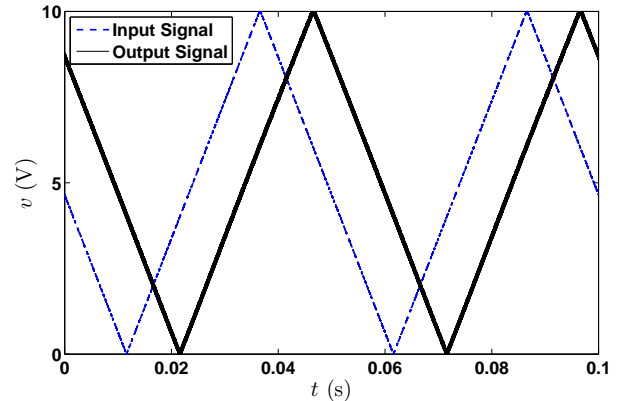


Fig. 5. Test signals of the delay block. Input signal (dashed line), and output signal (full line).

approximate the original Mackey-Glass equation. By means of the Kirchoff's law applied to the entire circuit shown in Fig. 1 we obtain

$$\frac{dv_c(t)}{dt} = \frac{1}{RC} \left[f \left(v_c \left(T_s \left\lfloor \frac{t}{T_s} - N + 1 \right\rfloor \right) \right) - v_c \right]. \quad (8)$$

The output of the delay block remains constant in each clock period, so it seems natural to solve Eq. 8 in steps. Let us solve

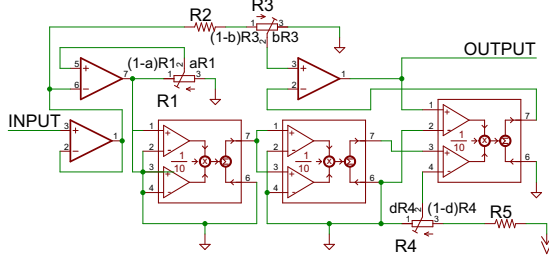


Fig. 6. Circuit schematics of the nonlinear function. $R_1 = 20 \text{ k}\Omega$, $R_2 = 56\text{k}\Omega$, $R_3 = 20\text{k}\Omega$, $R_4 = 2\text{k}\Omega$, $R_5 = 56\text{k}\Omega$

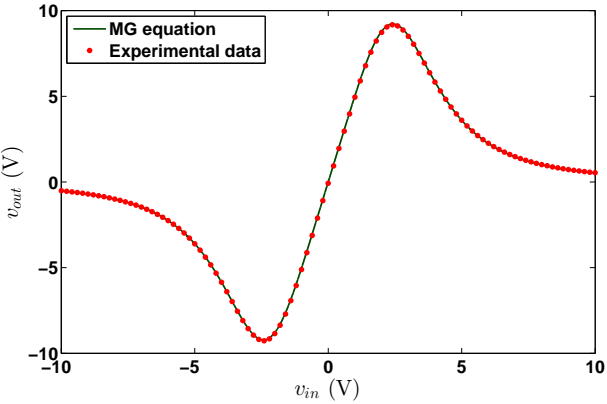


Fig. 7. Input-output of the function block, experimental data (red dots) and Eq. 3 (green line). Parameter values: $\beta = 525V^4$ and $\theta = 3.19V$

it, then, for $jT_s \leq t < (j+1)T_s$ and let $v_i = v_c(iT_s)$, then

$$\frac{dv_c}{dt}(t) = \frac{1}{RC} [f(v_{j-N+1}) - v_c]. \quad (9)$$

Since $f(v_{j-N+1})$ is constant, this equation can be readily solved, the solution knowing the value of v_c in $t = jT_s$ is

$$v_c(t) = (v_j - f(v_{j-N+1})) e^{\frac{nT_s-t}{RC}} + f(v_{j-N+1}). \quad (10)$$

Setting $t = (j+1)T_s$ and substituting the expression for $f(v)$ given in Eq. 3 it results

$$v_{j+1} = v_j e^{\frac{-T_s}{RC}} + (1 - e^{\frac{-T_s}{RC}}) \beta \frac{v_{j-N+1}}{\theta^n + v_{j-N+1}^n}. \quad (11)$$

It can be easily seen that this discrete time effective equation approaches to the original continuous time equation, Eq. 5, when N grows to infinity.

IV. SIMULATIONS AND RESULTS

To compare the solutions of the original (continuous-time) model with the effective (discrete-time) model, we performed simulations of both with the same parameters values. The original equation was simulated using a 5th order Runge-Kutta scheme with variable time step. Since N tending to infinity would reconstruct the original equation, the effective equation was simulated using the less favorable case, $N = 396$, and

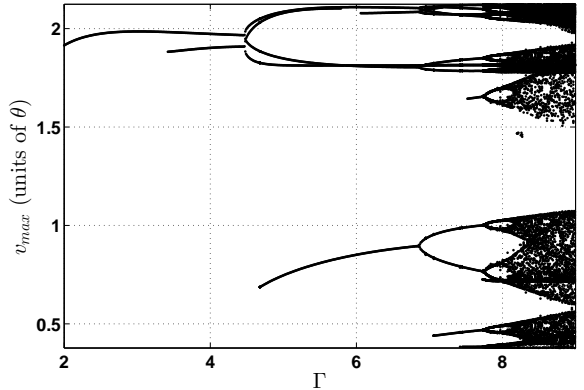


Fig. 8. Bifurcation diagram as a function of the time delay corresponding to the continuous-time simulations. Parameter values: $n = 4$ and $\alpha = 3.73$.

assumed that other values of N perform better than this value. For the circuit we used $N = 1194$, where we measured the voltage immediately after the delay block, and reconstructed the voltage in the capacitor with a tuned digital filter.

Bifurcation diagrams were obtained by plotting the maximum of temporal series, as a function of Γ , which is τ in units of RC . Such diagrams are shown in Figs. 8 and 9 respectively for simulations of original equation and effective equation, while experimental results are shown in Fig. 10. We can observe great agreement in all cases. The three figures present a typical behavior of DDEs: single branches that appear (*out of the blue*) or disappear for certain control parameter values. In addition, the familiar, already present in ODEs, period-doubling branches and chaotic behavior also emerge as the control parameter Γ is increased. These results are in agreement with previous works [2].

Some examples of time series with different Γ values are shown in Fig. 11 and 12, corresponding to the values indicated by vertical dashed lines in Figs. 9 and 10. These time series also show a great deal of concordance between experimental and simulated data. The first presented waveforms (*a1* and *a2*) correspond to a simple oscillation with only one peak per period. Increasing the time delay, Γ , after new peak appearances and a bifurcation, a more complex waveform, with longer period is observed (*b1* and *b2*). With additional increases in the time delay longer periods appear as shown in *c1* and *c2*. Finally, chaotic behavior, in agreement with the previous works [1], [9], [2], is seen in *d1* and *d2*.

V. CONCLUSION AND PERSPECTIVES

The Mackey-Glass model was simulated using an electrical analog. A novel approach was proposed to implement the function and delay blocks exhibiting several advantages compared with previous implementations. An exact equation for the electric evolution can be easily written thanks to the exact transfer function of the delay block. The parameter n is exactly determined by means of multipliers and divisors. The ordering of the blocks, which is usually ignored, played an important role in getting the most out of the delay block,

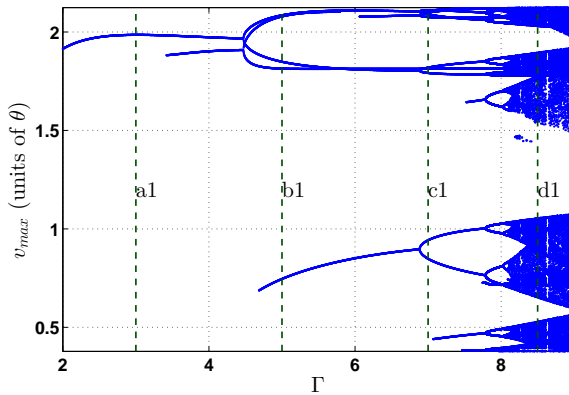


Fig. 9. Discrete time version of the bifurcation diagram shown in Fig.8 with $N = 396$. The vertical lines labeled with a_1 , b_1 , c_1 and d_1 correspond to the temporal series shown in Figs. 11 and 12.

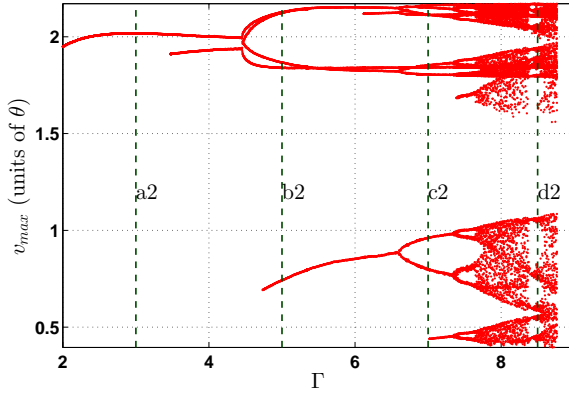


Fig. 10. Experimental results $n = 4$, $\alpha = 3.73$ and $N = 1194$. The labels a_2 , b_2 , c_2 and d_2 correspond to the temporal series shown in Figs. 11 and 12.

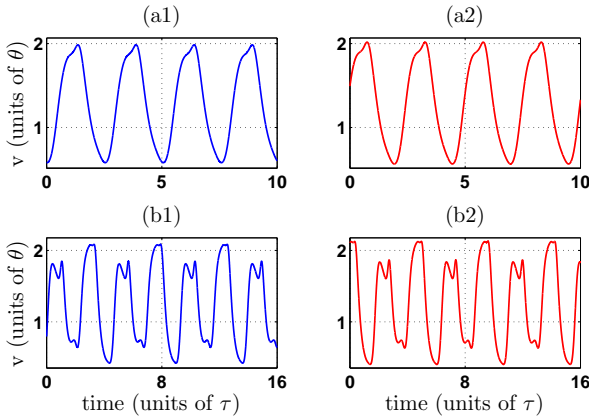


Fig. 11. Exemplary temporal evolutions of MG model, simulations (left and blue), and experiments (right and red). Parameter values: $\Gamma = 3$ (a) and $\Gamma = 5$ (b).

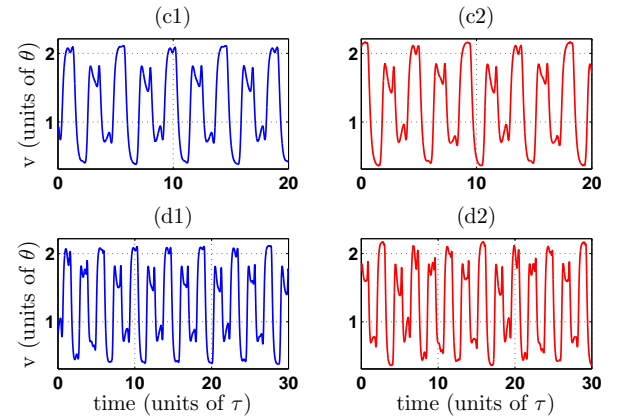


Fig. 12. Exemplary temporal evolutions of MG model, simulations (left and blue), and experimental data (right and red). Parameter values: $\Gamma = 7$ (c) and $\Gamma = 8.5$ (d).

and allowed to suppress a most of the electrical noise in the experimental data.

The results of numerical simulations of the the original equation were compared with the effective (discrete) equation and with the experimental data. According to the value of the time delay the system exhibits a wide variety of behaviors including fixed, periodic waveform with different numbers of peaks per period and, finally, aperiodic or chaotic solutions. The great agreement between experimental and numerical results suggests that can deeper understanding of the dynamics of MG model can be obtained using our implementation. In addition, this approach could be extended to other time-delayed systems.

ACKNOWLEDGMENT

The authors would like to thank CSIC (UdelaR) and PEDECIBA (Uruguay).

REFERENCES

- [1] M. C. Mackey and L. Glass, "Oscillation and chaos in physiological control systems," *Science*, vol. 197, no. 4300, pp. 287–289, 1977.
- [2] L. Junges and J. A. Gallas, "Intricate routes to chaos in the mackey-glass delayed feedback system," *Physics Letters A*, vol. 376, no. 18, pp. 2109–2116, 2012.
- [3] E. Shahverdiev, R. Nuriev, R. Hashimov, and K. Shore, "Chaos synchronization between the mackey-glass systems with multiple time delays," *Chaos, Solitons & Fractals*, vol. 29, no. 4, pp. 854–861, 2006.
- [4] L. Berezansky and E. Braverman, "Mackey-glass equation with variable coefficients," *Computers & Mathematics with Applications*, vol. 51, no. 1, pp. 1–16, 2006.
- [5] S. Sano, A. Uchida, S. Yoshimori, and R. Roy, "Dual synchronization of chaos in mackey-glass electronic circuits with time-delayed feedback," *Phys. Rev. E*, vol. 75, p. 016207, Jan 2007. [Online]. Available: <http://link.aps.org/doi/10.1103/PhysRevE.75.016207>
- [6] A. Namajūnas, K. Pyragas, and A. Tamaševičius, "Stabilization of an unstable steady state in a mackey-glass system," *Physics Letters A*, vol. 204, no. 3, pp. 255–262, 1995.
- [7] P. Grassberger and I. Procaccia, "Measuring the strangeness of strange attractors," *Physica D: Nonlinear Phenomena*, vol. 9, no. 1, pp. 189–208, 1983.
- [8] ———, "Estimation of the kolmogorov entropy from a chaotic signal," *Physical review A*, vol. 28, no. 4, pp. 2591–2593, 1983.

- [9] A. Namajūnas, K. Pyragas, and A. Tamaševičius, “An electronic analog of the mackey-glass system,” *Physics Letters A*, vol. 201, no. 1, pp. 42–46, 1995.
- [10] A. Kittel, J. Parisi, and K. Pyragas, “Generalized synchronization of chaos in electronic circuit experiments,” *Physica D: Nonlinear Phenomena*, vol. 112, no. 3, pp. 459–471, 1998.
- [11] A. Wan and J. Wei, “Bifurcation analysis of mackey–glass electronic circuits model with delayed feedback,” *Nonlinear Dynamics*, vol. 57, no. 1–2, pp. 85–96, 2009.
- [12] M. Tateno and A. Uchida, “Nonlinear dynamics and chaos synchronization in mackey-glass electronic circuits with multiple time-delayed feedback,” *Nonlinear Theory and Its Applications, IEICE*, vol. 3, no. 2, 2012.



Pablo Amil Pablo Amil received his bachelor degree from the University of the Republic, Uruguay, in 2012. Where he is currently finishing a master degree. His current research include nonlinear dynamics, and musical audio synthesis.



Cecilia Cabeza Cecilia Cabeza is associate professor in Physics at the Republic University (Uruguay). Her research interests have focused on nonlineal physics, chaos, fluids, and teaching of experimental physics. Cecilia holds a doctorate cotutelle from the Republic University (Uruguay) and the Paris VII University (France) in 2000.



Arturo C. Martí Arturo Martí is associate professor in Physics at the Republic University (Uruguay). His research interests have centred on traditional academic topics as chaos, turbulence, and complex networks but also include science popularization and teaching of physics using everyday tools. Arturo obtained his degree in 1992 from the Republic University (Uruguay) and his PhD from Barcelona University (Spain) in 1997.